BURST-BY-BURST ADAPTIVE JOINT DETECTION CDMA

E. L. Kuan, C. H. Wong and L. Hanzo

Department of Electronics and Computer Science,
University of Southampton, Southampton S017 1BJ, UK.
Tel: +44-703-593 125, Fax: +44-703-594 508
Email:lh@ecs.soton.ac.uk http://www-mobile.ecs.soton.ac.uk

Abstract - Adaptive Quadrature Amplitude Modulation (AQAM) is combined with Joint Detection Code Division Multiple Access (JD-CDMA) in order to increase the throughput of a communications system, while maintaining a target BER. The QAM modes are adaptively switched, by estimating the Signal to Interference plus Noise Ratio (SINR) at the output of the joint detection receiver. For an eight-user AQAM/JD-CDMA scheme, a BPS performance of about 3.5 bits/symbol is achieved at an average SNR of about 18 dB, with a BER of approximately 0.02%, when using three different modulation modes, namely BPSK, 4-QAM and 16-QAM.

I. INTRODUCTION

Burst-by-burst Adaptive Quadrature Amplitude Modulation (AQAM) [1, 2] is a technique that attempts to increase the throughput of the system by switching between modulation modes depending on the state of the mobile channel, which often exhibits deep fades resulting in error bursts. Therefore, the modulation mode can be adaptively switched between each transmission burst, in order to maintain a given target BER, while providing a time-variant bits per symbol (BPS) throughput, by using a modulation mode with a higher number of constellation points, when the channel is favourable, and switching to a lower number of points, when the channel is hostile.

In order to determine the choice of modulation mode for the next transmission burst, we have to estimate the quality of the channel, which the burst to be transmitted will be exposed to. This parameter is then estimated at the receiver due to assuming reciprocity of the channel and the chosen modulation mode is communicated to the remote receiver in a closed loop scheme, or estimated in an open-loop scheme. The latter regime is typically applicable to Time Division Duplex (TDD) schemes, where the uplink and downlink use the same frequency. Hence, it can be argued that the uplink and downlink experience similar channel fading conditions, separated by half a TDD frame, as long as the transmission bandwidth is sufficiently narrow for non-frequency-selective channel conditions to hold. The AQAM principles were also extended to wideband propagation conditions upon defining a channel quality metric on the basis of the mean-squared error (MSE) at the output of the channel equalizer, which was then used to control the choice of the modem modes for each transmitter burst [3].

In the context of CDMA, the uplink transmissions from different mobile stations have independent channels, while in the downlink, each mobile station is affected only by the channel between the base station and itself. Therefore, a closed loop scheme is needed to transmit the modulation mode information. AQAM schemes perform most successfully, when the fading in a channel varies slowly compared to the TDD frame duration, since then the channel estimate based on the received burst will be more up-to-date at half a TDD frame offset, when transmission takes place. Hence the above channel estimation regime is less accurate in a fast-fading channel and this renders the choice of modulation mode less appropriate at the time of transmission. TDD/CDMA systems have been proposed by Miya *et al* [4] and Jeong *et al* [5]. They showed that the close correlation between the downlink and uplink transmissions could be used to implement transmission and reception space diversity at the base station, as well as open-loop power control. This leads us to conclude that this correlation can also be exploited in AQAM/CDMA systems. For example, the uplink transmission can be utilized to estimate the expected channel quality for downlink transmissions due to this close correlation, leading to an adequate choice of the modulation mode. By contrast, the receiver at either end of a duplex link can communicate its perception of the channel quality to the transmitter in a closed-loop fashion, in order to request the most appropriate transmission mode to be used.

Joint Detection Code Division Multiple Access (JD-CDMA) receivers [6] are multiuser detectors developed for synchronous burst transmissions that mitigate the effects of inter-symbol interference (ISI) caused by dispersive wideband channels and by the multiple access interference (MAI) inherent in CDMA transmissions. The implementation of the joint detection receivers is independent of the modulation mode used, since the receiver simply inverts the associated system matrix and invokes a decision concerning the received symbol, irrespective of how many bits per symbol were used. **Therefore, joint detection receivers are amenable to amalgamation with AQAM, since they do not have to be reconfig-**

0-7803-5565-2/99/$10.00 © 1999 IEEE

ured each time the modulation mode is switched.

Previous research in AQAM schemes for TDMA transmissions have also been carried out by Sampei *et al* [7] and Goldsmith *et al* [8]. In parallel, previous work in the field of JD-CDMA was hallmarked, for example, by the contributions of Klein *et al* [6]. This paper proposes to combine AQAM with JD-CDMA and hence to increase the system's throughput in terms of bits per symbol (BPS).

II. JOINT DETECTION

Joint detection receivers [6] are a class of multiuser receivers that were developed based on equalization techniques [1] used for mitigating the effects of inter-symbol interference (ISI). These receivers utilize the channel impulse response (CIR) estimates and the spreading sequences of all the users in order to reduce the level of multiple access interference (MAI) in the processed signal.

By concatenating the data symbols of each CDMA user successively, as though they were transmitted by one user, we can visualize the similarities between ISI and MAI and apply the principles of conventional TDMA-oriented channel equalization [1] to multiuser detection. The concatenated data vector is thus :

$$\mathbf{d} = d_1^1, d_2^1, \ldots, d_N^1; d_1^2, d_2^2, \ldots, d_N^2; \ldots, d_1^K, \ldots d_N^K, \quad (1)$$

where $\mathbf{d}$ represents the data frame and d_n^k represents the n-th symbol of the k-th user for $n = 1, 2, \ldots N$ and $k = 1, 2, \ldots K$.

Again, in order to perform joint detection, a system matrix, $\mathbf{A}$, is constructed using the CIR estimates and spreading sequences of all the K users. This matrix represents the combined effect of the spreading sequences and channel responses on the data vector in Equation 1. For each data symbol in $\mathbf{d}$, the combined channel response that affected it is constructed by convolving the channel estimates and the spreading sequence used for that symbol. In order to simplify our discussions, it is assumed that for a given user, the same spreading sequence is used for all the data symbols in the same transmission burst and the CIR varies slowly, such that the CIR estimates remain constant throughout the data burst. Therefore, the combined impulse response for each user can be represented as :

$$\mathbf{b}^{(k)} = \mathbf{c}^{(k)} * \mathbf{h}^{(k)}, \quad (2)$$

where the combined impulse response, $\mathbf{b}^{(k)}$, is defined by the convolution of the user's signature sequence, $\mathbf{c}^{(k)}$, and the channel estimates, $\mathbf{h}^{(k)}$.

In order to construct the system matrix $\mathbf{A}$, the combined impulse responses, $\mathbf{b}^{(k)}$, are arranged according to:

$$[\mathbf{A}]_{ij} = \begin{cases} b_l^{(k)} & \text{for } k = 1, \ldots, K; \quad n = 1, \ldots, N; \\ & l = 1, \ldots, Q + W - 1 \\ 0 & \text{otherwise,} \end{cases} \quad (3)$$
$$\text{for } i = 1, \ldots, NQ + W - 1, \quad j = 1, \ldots, KN,$$

where $i = Q(n-1) + l$ and $j = n + N(k-1)$. The limits of i and j are $i = 1, \ldots, NQ + W - 1$ and $j = 1, \ldots, KN$ respectively, and the symbols Q, K and N represent the spreading sequence length in chips, the total number of users and the number of data symbols transmitted per user, repsectively. The notation $[\mathbf{A}]_{ij}$ represents the element in the i-th row and j-th column of the matrix $\mathbf{A}$ and $b_l^{(k)}$ denotes the l-th element of the vector $\mathbf{b}^{(k)}$.

The joint detector chosen for our work was the Minimum Mean Square Error Block Decision Feedback Equalizer (**MMSE-BDFE**). The principle behind MMSE estimation is the minimization of the error between the data estimate, $\hat{\mathbf{d}}$, and the actual data, $\mathbf{d}$, hence the MMSE estimator minimizes the quadratic expression [6] :

$$Q(\hat{\mathbf{d}}) = E[(\mathbf{d} - \hat{\mathbf{d}})^H (\mathbf{d} - \hat{\mathbf{d}})]. \quad (4)$$

Using the Orthogonality Principle [9], it can be shown that the **linear** MMSE joint detector estimates $\mathbf{d}$ according to :

$$\hat{\mathbf{d}} = (\mathbf{A}^H \mathbf{R}_n^{-1} \mathbf{A} + \mathbf{R}_d^{-1})^{-1} \mathbf{A}^H \mathbf{R}_n^{-1} \mathbf{y}, \quad (5)$$

where $\mathbf{y}$ is the vector of the composite received signal due to the transmissions of all users to the JD-CDMA receiver, $\mathbf{R}_n^{-1}$ is the noise covariance matrix and $\mathbf{R}_d^{-1}$ is the data covariance matrix. In Equation 5, the vector $\mathbf{y}$ is first passed through a whitening matched filter process, which is represented by the matrix $(\mathbf{A}^H \mathbf{R}_n^{-1})$. The resultant vector is then multiplied with the inverse of the matrix $(\mathbf{A}^H \mathbf{R}_n^{-1} \mathbf{A} + \mathbf{R}_d^{-1})$, where the matrix $(\mathbf{A}^H \mathbf{R}_n^{-1} \mathbf{A})$ represents the cross-correlation matrix of the different users after passing through the matched filtering process.

In the MMSE-BDFE algorithm, Cholesky decomposition [10] is performed on the matrix of $(\mathbf{A}^H \mathbf{R}_n^{-1} \mathbf{A} + \mathbf{R}_d^{-1})$, resulting in a lower triangular and upper triangular matrix of $\mathbf{L}$ and $\mathbf{U}$ respectively, where

$$\mathbf{A}^H \mathbf{R}_n^{-1} \mathbf{A} + \mathbf{R}_d^{-1} = \mathbf{L}\mathbf{U}. \quad (6)$$

The matrix $\mathbf{L}^{-1}$ is used as the feed-forward matrix to remove some of the interference in the signal. The data estimates are then fed back into the detector using the elements in the matrix $\mathbf{U}$ as the feedback filter tap coefficients. The block diagram of the MMSE-BDFE is depicted in Figure 1. Again, the received vector is first processed with a whitening matched filter matrix, $(\mathbf{A}^H \mathbf{R}_n^{-1})$. Next, the resultant vector is multiplied with the feed-forward matrix of $\mathbf{L}^{-1}$. The feedback process in the Figure can be expressed as :

$$d_i' = \frac{\hat{y}_i - \sum_{j=i+1}^{J=KN} U_{i,j} \hat{d}_j}{U_{i,i}}, \quad (7)$$

where d_i' is the i-th data estimate of the data vector $\mathbf{d}$, $\hat{d}_i$ is the i-th data symbol that has been quantized by the data detector, $\hat{y}_i$ is the i-th element of the vector $\hat{\mathbf{y}}$ at the output of the feed-forward filter and $U_{i,j}$ is the element in the i-th row and j-th column of the matrix $\mathbf{U}$.

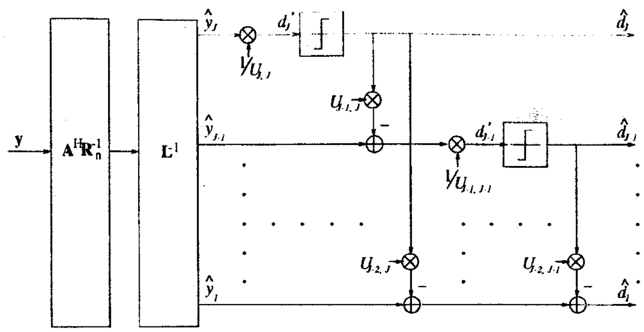

Figure 1: **MMSE-BDFE** used for burst-by-burst adaptive synchronous JD-CDMA reception

III. SYSTEM OVERVIEW

Figure 2 shows the typical variation of Signal to Interference plus Noise Ratio (SINR) for each of the two users in our experimental two-user system at the output of the **MMSE-BDFE** [6] and the corresponding number of bit errors in a transmission burst using 4-QAM. The Figure shows that not only does the output SINR vary over time, but that the variation in output SINR is different for different users. Since AQAM exploits the variability in the channel quality, these Figures suggest that it is promising to combine AQAM with JD-CDMA.

The system concept was tested, employing various number of users, with each user transmitting over an independently fading 7-path COST 207 Bad Urban channel [11]. A profile of the channel is shown in Figure 3. Each path was faded independently using Rayleigh fading with a Doppler frequency of $f_D = 80$ Hz and a Baud rate of $R_b = 2.167$ MBaud. The power fluctuations due to path loss and shadowing were assumed to be eliminated by power control. The noise, $\mathbf{n}$, was assumed to be additive white Gaussian noise (AWGN) with zero mean and a covariance matrix of $\sigma^2\mathbf{I}$, where σ^2 is the variance of the noise. The burst structure used in the simulations mirrored the spread/speech burst structures proposed in the so-called FMA1 mode of the Pan-European FRAMES proposal [12]. The MMSE-BDFE was used as the multiuser receiver and perfect decision feedback was assumed. The Signal to Interference plus Noise ratio (SINR), $\gamma(k,n)$ at the output of the MMSE-BDFE was estimated, by assuming perfect CIR estimation according to Reference [6]. For the n-th symbol of the k-th user :

$$\gamma(k,n)| = g^2[\mathbf{D}]^2_{j,j} - 1, \tag{8}$$

where $n = 1,\ldots,N$, $k = 1,\ldots,K$, $j = n+N(k-1)$ and g^2 is the gain or attenuation of the transmitted signal. $\mathbf{D}$ is a diagonal matrix with real-valued elements obtained from the matrix $\mathbf{U}$ in Equation 6 such that $\mathbf{DU'} = \mathbf{U}$, and $\mathbf{U'}$ is also an upper triangular matrix where all the elements on its main diagonal have values of one. Due to space considerations, a detailed derivation is avoided but the reader is referred to the references cited for a more comprehensive discussion. Using the output SINR calculated for each transmission burst, the appropriate modulation mode was chosen from the set of legitimate modes, as it is highlighted below.

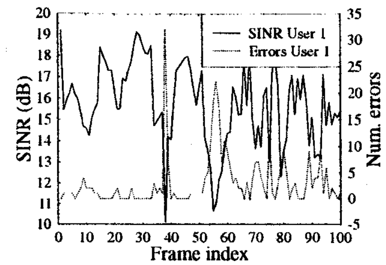

(a) User 1

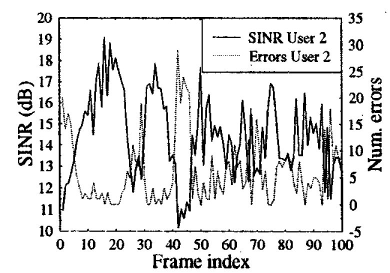

(b) User 2

Figure 2: Comparison of the SINR of consecutive transmission frames at the output of the **MMSE-BDFE** for two different users over the same period of time. The number of errors per 4-QAM transmission burst corresponding to the SINR is also shown. The COST 207 Bad Urban CIR [11] was employed using the normalised Doppler frequency of $f_D = 80$ Hz.

IV. SYSTEM PERFORMANCE

In our work, three modulation modes were used, namely BPSK, 4-QAM and 16-QAM. The conditions used to switch between the three modes were set according to their SINR requirements as :

$$\text{Mode} = \begin{cases} \text{BPSK} & \text{for } \gamma_o(k) < t_1 \\ \text{4-QAM} & \text{for } t_1 \leqslant \gamma_o(k) < t_2 \\ \text{16-QAM} & t_2 \leqslant \gamma_o(k) \end{cases}, \tag{9}$$

where $\gamma_o(k) = \frac{1}{N}\sum_{n=1}^{N}\gamma(k,n)$, and $\gamma_o(k)$ is the average SINR of the k-th user at the output of the MMSE-BDFE. Initially, a set of simulations was invoked, setting $t_1 = 12$ dB and $t_2 = 18$ dB, and another experiment employed

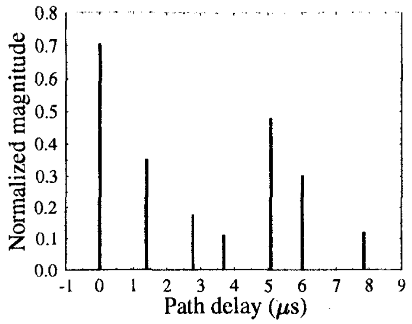

Figure 3: Normalized channel impulse response for a seven path Bad Urban channel [11].

$t_1 = 8$ dB and $t_2 = 14$ dB. The results of these simulations are shown in Figure 4. In the Figure, the BER performance and the throughput, measured in terms of the average number of bits-per-symbol (BPS) are shown. Explicitly, on the vertical axis at the left, the BER is scaled, while at the right, the BPS. The BPS for BPSK, 4-QAM and 16-QAM is constant, namely 1, 2 and 4 BPS, respectively and hence not plotted in the Figure. By looking at the BER curves for the fixed modulation modes of 4-QAM and 16-QAM, it can be seen that for achieving an average BER of 10^{-2}, the E_b/N_0 values required for 4-QAM and 16-QAM are approximately 12 dB and 18 dB, respectively. Therefore, the initial set of thresholds of $t_1 = 12$ dB and $t_2 = 18$ dB were chosen.

The general trend is that the BER of fixed modulation schemes improves as the average SNR is increased, since the error events are more probable when the instantaneous burst SNR is low. By contrast, our proposed AQAM/JD-CDMA scheme can vary the number of BPS, in order to maintain a near-constant target BER. When the average SNR improves, the average throughput in BPS also improves. Considering the results of Figure 4, we can see that for the first set of thresholds $\{t_1 = 12 \text{ dB}, t_2 = 18\}$, although the BER performance was good, the increase in throughput did not match the potential 4 BPS offered by the system. This was because the thresholds were set at a relatively high level, thus lowering the probability of the higher-order modulation modes being used. A second set of thresholds was then chosen, i.e. the values of $t_1 = 8$ and $t_2 = 14$ dB respectively. For this set of threshold values, the Figure shows that at low E_b/N_0 values, the BER performance of the AQAM system was slightly better than that of BPSK, because the inclusion of higher bit-rate modes allowed a higher number of bits to be transmitted when the channel quality was good. This caused an overall decrease in the average BER. Observe in Figure 5 that as the E_b/N_0 increased, the BER curve of the AQAM system crossed over the fixed-mode BPSK curve and approached that of 4-QAM and eventually 16-QAM at high E_b/N_0 values. The throughput performance of the system, measured in average bits per symbol (BPS) terms was also presented in the same Figure. As the E_b/N_0 increased, the average number of bits per symbol increased and at $E_b/N_0 = 17$ dB, the throughput achieved was approximately 3.6 bits per symbol, which approached the 4 bits per symbol offered by 16-QAM, while the BER was still lower than the BER achieved by the 16-QAM system. This was because when the channel quality dropped, the modulation mode could be switched to a lower-order one that provided a lower error probability, thus reducing the number of errors received at a concomitant reduction of the BPS capacity. Most of the information was transmitted, when the channel conditions were favourable, resulting in an improved BER performance. The probability of each mode being used in the simulation run for $t_1 = 8$ and $t_2 = 14$ dB is plotted in Figure 5.

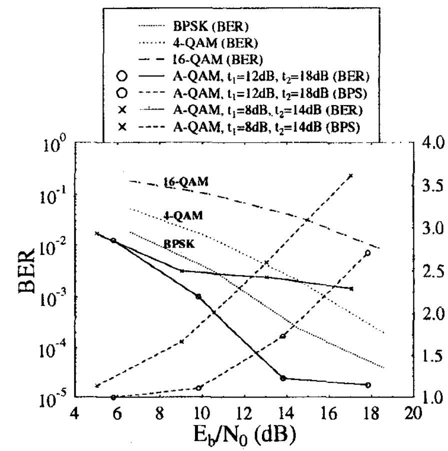

Figure 4: The average BER and BPS performance versus average SNR of a combined JD-CDMA/AQAM system for $K = 2$ users. Three modulation modes were used, namely BPSK, 4-QAM and 16-QAM. The modulation mode was switched by calculating the output SINR of the **MMSE-BDFE** individually for each user. Two different sets of thresholds were used, as shown in the legends. The BER curves for the same system but using fixed modulation modes of BPSK, 4-QAM and 16-QAM for $K = 2$ users are also shown.

The rest of the simulations were then conducted with the thresholds of $t_1 = 8$ dB and $t_2 = 14$ dB. The number of users in the system was increased from $K = 2$ to 4, 6 and 8 users. The results of these investigations are compared in Figure 6. Although the graphs appear slightly cluttered, it is beneficial to view all the curves comparatively in the same Figure. It can be seen that the trend in the BER and BPS curves are as expected, where the average BPS increases as E_b/N_0 increases. The modulation mode gradually shifts from BPSK to 4-QAM and 16-QAM at high E_b/N_0 values. As the number of users increase, the performance of the system degrades only slightly even

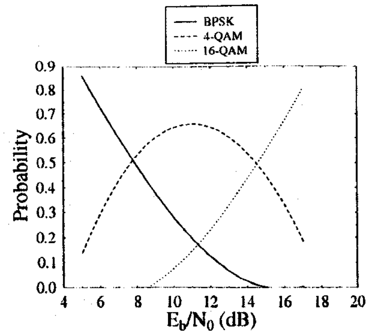

Figure 5: The probability of each modulation mode being chosen for transmission in a triple-mode (BPSK, 4-QAM, 16-QAM), two-user AQAM/JD-CDMA system.

though the interference increases. This is because the joint detection algorithm is capable of reducing the interference by using all the available knowledge concerning the CIR estimates and spreading sequences.

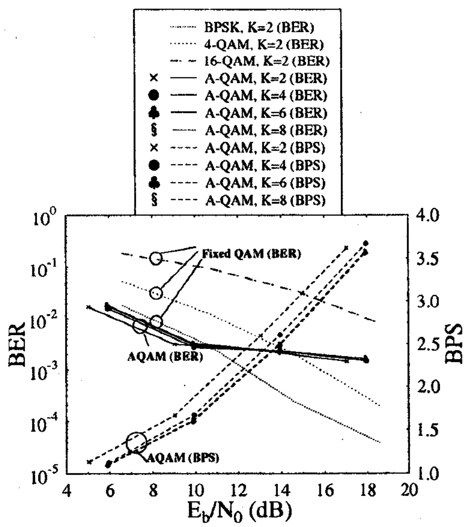

Figure 6: The average BER and BPS performance versus average SNR of a combined JD-CDMA/AQAM system for $K = 2$, 4, 6 and 8 users. Three modulation modes were used, namely BPSK, 4-QAM and 16-QAM. The BER curves for the same system but using fixed modulation modes of BPSK, 4-QAM or 16-QAM for $K = 2$ users are also shown.

V. CONCLUSIONS

The potential of AQAM-assisted JD-CDMA was demonstrated. It should also be noted that since the symbol-oriented JD receiver algorithms are independent of the number of bits per symbol, i.e. the modulation scheme used, there is no extra complexity incurred in the JD-CDMA receivers due to the changes in modulation modes. Our future work is concentrated on optimizing the switching regime in order to further improve the system's performance.

ACKNOWLEDGEMENT

The financial support of the European Union under the auspices of the Pan-European FIRST project and that of Motorola ECID, Swindon UK is gratefully acknowledged. The authors also wish to thank the members of the FIRST consortium for helpful discussions and for their friendship.

VI. REFERENCES

[1] W.T.Webb and L.Hanzo, "Modern Quadrature Amplitude Modulation : Principles and Applications for Fixed and Wireless Channels," , John Wiley and IEEE Press, London, 1994.

[2] , W.T.Webb and R.Steele "Variable Rate QAM for mobile radio," *IEEE Trans. on Comms.*, vol. 43, pp. 2223 - 2230, July 1995.

[3] , C.H.Wong and L.Hanzo "Upper-bound performance of a wideband burst-by-burst adaptive modem," *accepted for publication in the Proc. of the IEEE VTC'99*, .

[4] , K.Miya, O.Kato, K.Homma, T.Kitade, M.Hayashi and T.Ue "Wideband CDMA Systems in TDD-Mode operation for IMT-2000," *IEICE Trans. on Comms.*, vol. E81-B, pp. 1317-1326, July 1998.

[5] , I.Jeong and M.Nakagawa "A Novel Transmission Diversity System in TDD-CDMA," *IEICE Trans. on Comms.*, vol. E81-B, pp. 1409-1416, July 1998.

[6] , A.Klein, G.K.Kaleh and P.W.Baier "Zero forcing and minimum mean square error equalization for multiuser detection in code division multiple access channels," *IEEE Trans. on Vehic. Tech.*, vol. 45, pp. 276-287, May 1996.

[7] , S.Sampei, S.Komaki and N.Morinaga "Adaptive modulation/TDMA scheme for large capacity personal multimedia communications systems," *IEICE Trans. on Comms.*, vol. E77-B, pp. 1096-1103, September 1994.

[8] , A.J.Goldsmith and S.G.Chua "Variable Rate Variable Power MQAM for Fading Channels," *IEEE Trans. on Comms.*, vol. 45, pp. 1218 - 1230, October 1997.

[9] , A.D.Whalen "Detection of signals in noise," , Academic Press, 1971.

[10] , G.H.Golub and C.F.van Loan "Matrix Computations," , North Oxford Academic, 1983.

[11] , "COST 207 : Digital land mobile radio communications, final report," , Office for Official Publications of the European Communities, Luxembourg, 1989.

[12] , A.Klein, R.Pirhonen, J.Sköld and R.Suoranta "FRAMES Multiple Access Mode 1 - Wideband TDMA with and without spreading," *Proc. of the IEEE PIMRC'97*, pp. 37-41, 1997.